

UNCLASSIFIED

SECURITY CLASSIFICATION OF THIS PAGE

## REPORT DOCUMENTATION PAGE

1a. REPORT SECURITY CLASSIFICATION UNCLASSIFIED			1b. RESTRICTIVE MARKINGS	
2a. SECURITY CLASSIFICATION AUTHORITY			3. DISTRIBUTION/AVAILABILITY OF REPORT Approved for public release; distribution unlimited	
2b. DECLASSIFICATION/DOWNGRADING SCHEDULE				
4. PERFORMING ORGANIZATION REPORT NUMBER(S) NUSC TD 7855			5. MONITORING ORGANIZATION REPORT NUMBER(S)	
6a. NAME OF PERFORMING ORGANIZATION Naval Underwater Systems Center		6b. OFFICE SYMBOL (If applicable) 332	7a. NAME OF MONITORING ORGANIZATION	
6c. ADDRESS (City, State, and ZIP Code). New London Laboratory New London, CT 06320			7b. ADDRESS (City, State, and ZIP Code)	
8a. NAME OF FUNDING/SPONSORING ORGANIZATION Naval Material Command		8b. OFFICE SYMBOL (If applicable) 05B	9. PROCUREMENT INSTRUMENT IDENTIFICATION NUMBER	
8c. ADDRESS (City, State, and ZIP Code) Washington, DC 20360			10. SOURCE OF FUNDING NUMBERS	
			PROGRAM ELEMENT NO.	PROJECT NO. A70204
			TASK NO.	WORK UNIT ACCESSION NO.
11. TITLE (Include Security Classification) SCATTERING FROM MULTIPLE COMPLIANT TUBE GRATINGS IN A VISCOELASTIC LAYER				
12. PERSONAL AUTHOR(S) Ronald P. Radlinski and Robert S. Janus				
13a. TYPE OF REPORT		13b. TIME COVERED FROM TO	14. DATE OF REPORT (Year, Month, Day) 1987 January 13	15. PAGE COUNT 18
16. SUPPLEMENTARY NOTATION A paper presented at the 110 meeting of the Acoustical Society of America, November 1985, Nashville, Tennessee				
17. COSATI CODES			18. SUBJECT TERMS (Continue on reverse if necessary and identify by block number) Baffles Elastic Layers Compliant Tubes	
FIELD	GROUP	SUB-GROUP		
19. ABSTRACT (Continue on reverse if necessary and identify by block number)  From previous studies of scattering from multiple gratings of resonant compliant tubes in water [R. P. Radlinski and M. M. Simon, J. Acoust. Soc. Am., vol. 72 (1982)], the excitation of noncompliant, antisymmetric structural modes by nearfield evanescent waves was found to severely degrade the reflectivity of closely packed gratings in the bandwidth of excitation of the compliant symmetric modes. Also, transmission resonances due to the spring-mass-spring configuration of the two gratings separated by a fluid mass diminished low frequency performance. In this paper, encapsulating the gratings in a low-stiffness elastomer is shown experimentally to have a minimum effect on single and widely separated gratings with respect to fluid but enhances the performance of closely packed gratings. Comparison of insertion loss performance with a high stiffness encapsulant indicates dramatic differences in bandwidth and frequency response. A mathematical model will be discussed and compared with the experimental data.				
20. DISTRIBUTION/AVAILABILITY OF ABSTRACT <input type="checkbox"/> UNCLASSIFIED/UNLIMITED <input checked="" type="checkbox"/> SAME AS RPT. <input type="checkbox"/> DTIC USERS			21. ABSTRACT SECURITY CLASSIFICATION UNCLASSIFIED	
22a. NAME OF RESPONSIBLE INDIVIDUAL Ronald P. Radlinski			22b. TELEPHONE (Include Area Code) (203) 440-4546	22c. OFFICE SYMBOL 332

NUSC Technical Document 7855  
13 January 1987

LIBRARY  
RESEARCH REPORTS DIVISION  
NAVAL POSTGRADUATE SCHOOL  
MONTEREY, CALIFORNIA 93940

# **Scattering From Multiple Compliant Tube Gratings in A Viscoelastic Layer**

**A Paper Presented at the  
110th Meeting of the Acoustical Society of America,  
November 1985, Nashville, Tennessee**

Ronald P. Radlinski  
Robert S. Janus  
Surface Ship Sonar Department



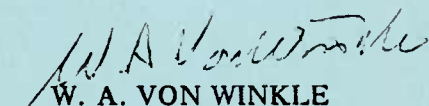
**Naval Underwater Systems Center**  
**Newport, Rhode Island / New London, Connecticut**

JANUARY 1987,

## PREFACE

This document was prepared under NUSC IR/IED Project No. A70204, "Scattering From Elastic Shells," Principal Investigator, R. P. Radlinski (Code 332). The Sponsoring Activity was Naval Material Command (Code 05B), CAPT Z. L. Newcomb, Navy Project No. ZN00001.

REVIEWED AND APPROVED: 13 January 1987

  
W. A. VON WINKLE  
ASSOCIATE TECHNICAL DIRECTOR  
FOR RESEARCH AND TECHNOLOGY

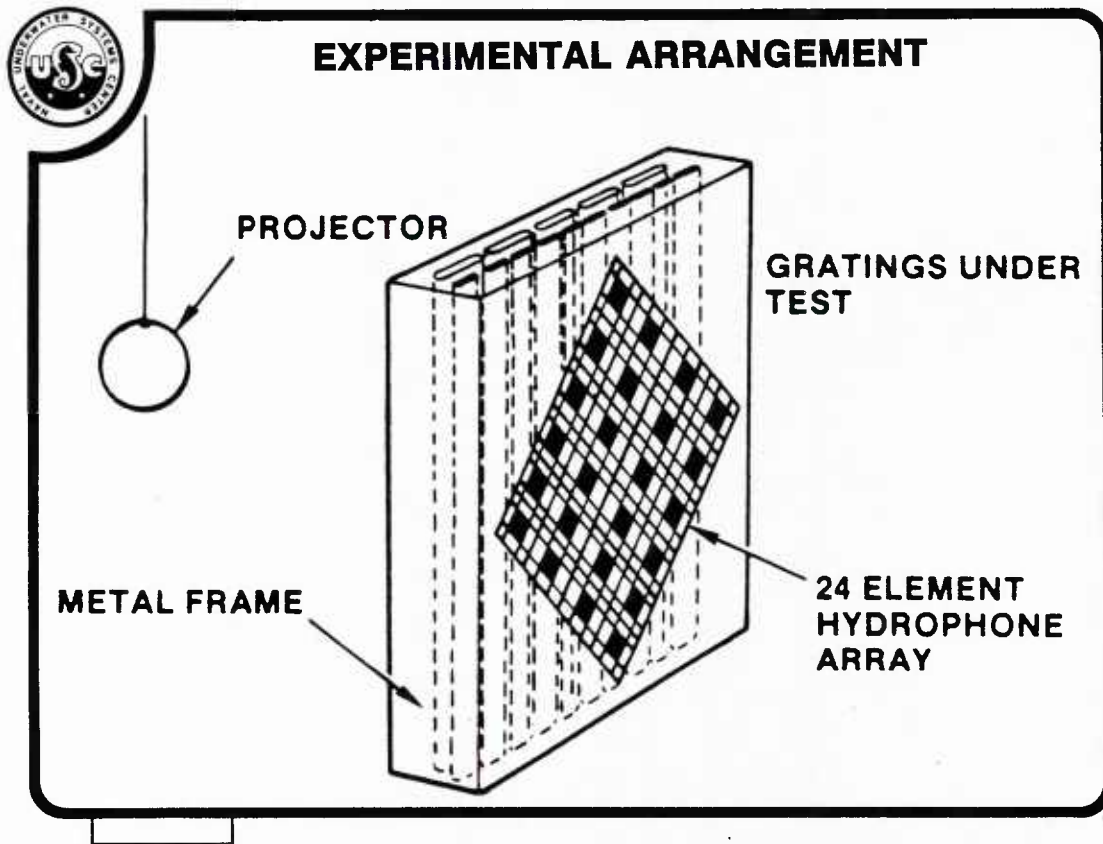
DESTRUCTION NOTICE -- For classified documents, follow the procedures in DoD 5200.22-M, Industrial Security Manual, Section 11-19, or DoD 5200.1-R, Information Security Program Regulation, Chapter IX. For unclassified, limited documents, destroy by any method that will prevent disclosure of contents or reconstruction of the documents.

## SCATTERING FROM MULTIPLE COMPLIANT TUBE GRATINGS IN AN ELASTIC LAYER

### INTRODUCTION

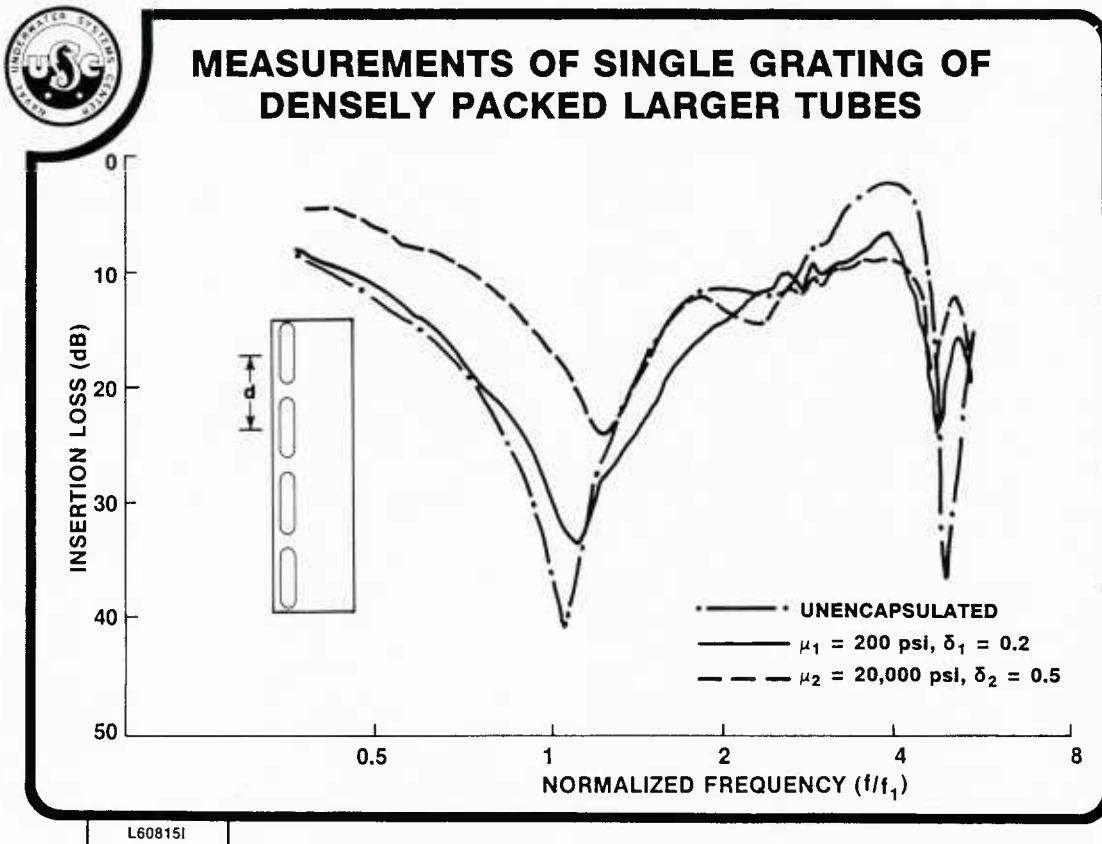
Compliant tubes are used as reflecting baffles. Their pressure release characteristics are the result of a net volume velocity associated with structural bending modes that are symmetric about the major and minor axes of the tubes. In this paper, the interactions between gratings of tubes encapsulated in two elastomers that have shear moduli which differ by two orders of magnitude will be investigated. The spacing between gratings are important because of evanescent waves which can excite noncompliant structural modes that degrade the performance of the baffle. Typically each grating is composed of a different sized tube to enhance the bandwidth of decoupling. Placing the grating in a suitable elastomer provides a means of minimizing the effects of the evanescent waves.

The first section of this presentation will compare experimental data of tubes in fluid versus tubes in elastic layers. The second part discusses a two dimensional theoretical model that includes propagation of both dilatational and shear waves in the elastic layer with compliant tube inclusions. Comparisons of the calculation from the model with the experimental data are discussed in the third section.



VIEWGRAPH 1

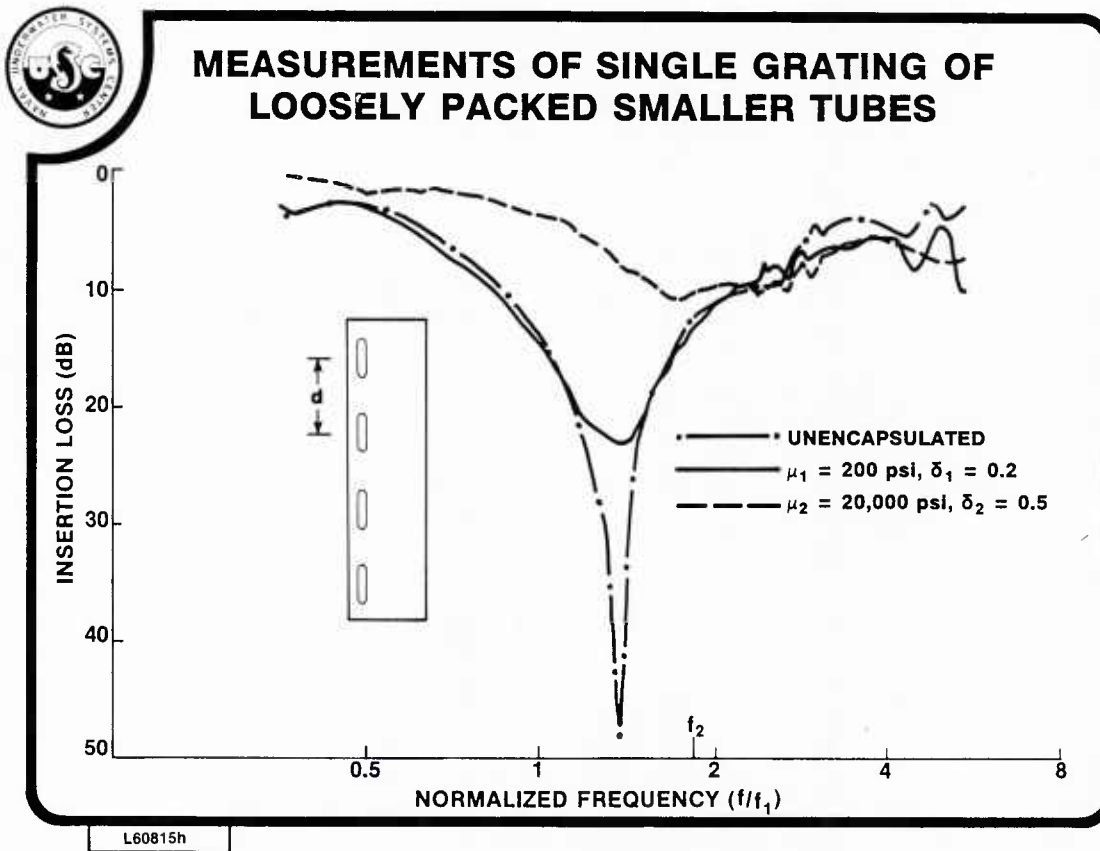
To measure insertion loss, an unshaded twenty-four element array was used as the receiver to discriminate against diffraction around the gratings and to average residual evanescent waves. Diffraction was further reduced by positioning the array diagonally with respect to the rectangular panels. Initially the array was used to measure the incident field without the tubing. The gratings were then inserted between the source and receiver and the transmitted pressure relative to the incident pressure was determined. Insertion loss is defined here as  $20 \log (\text{incident pressure}/\text{transmitted pressure})$ . A large insertion loss implies the transmitted energy is small. For the configurations that will be considered, the grating spacing is always less than a wavelength in water, thus only one wave propagates outside the elastomer with a direction normal to the gratings. The other waves are evanescent in the sense that they propagate parallel to the grating but decay rapidly in a direction normal to the gratings.



VIEWGRAPH 2

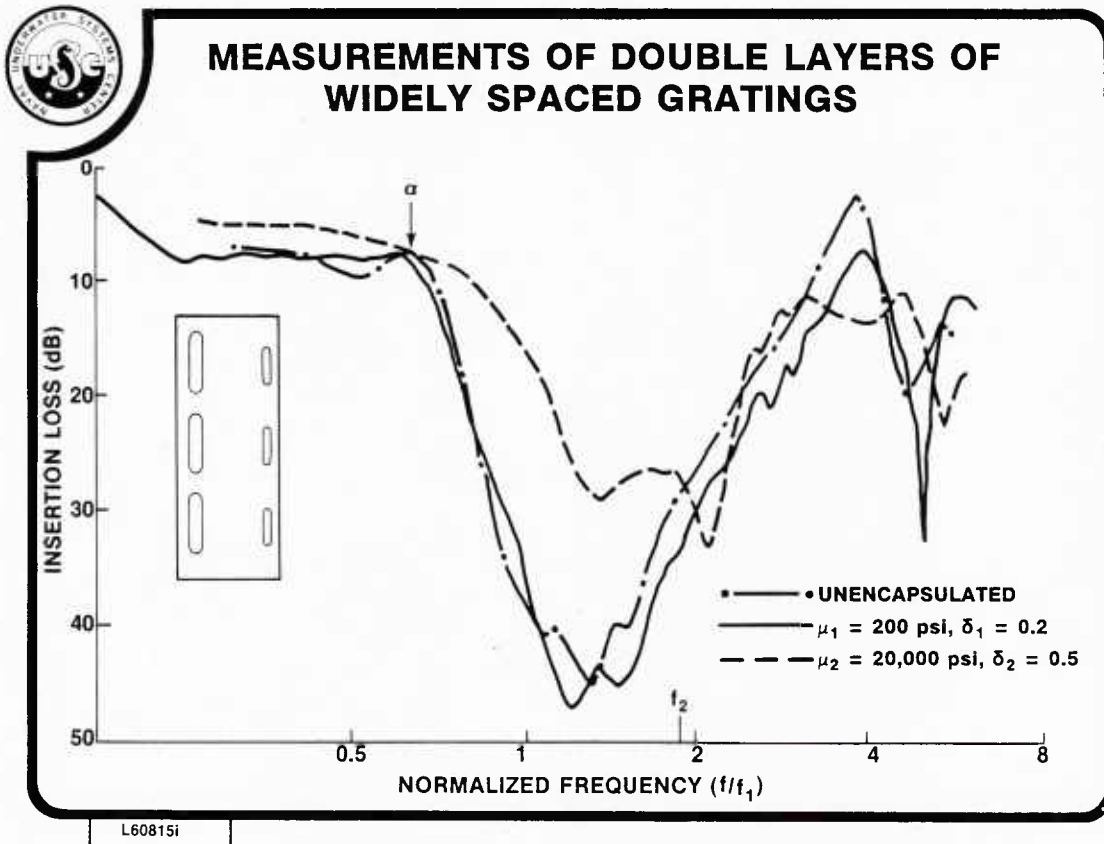
The measured normal incidence insertion loss for a single grating to be used later in combined multiple gratings is presented to show the stiffness effect of an encapsulant as a function of the shear modulus. The frequency axis is normalized to the in-air resonance frequency ( $f_1$ ) of the first compliant bending mode. The tubes are steel oval shells and have an aspect ratio of major to minor axis of about 7.5. The static compliance is about 200 times that of water. When the tubes are encapsulated in a low stiffness elastomer, the locations of insertion loss maxima do not change significantly but the depth decreases because of the damping factor. As the stiffness and damping increase, the character of the insertion loss changes dramatically. The additional stiffness on the tubes increases the effective resonance frequency of the structural modes. The stiffness also decreases the vibrational motion so that more energy tends to be transmitted through the layer. The increased insertion loss at about  $5.5f_1$  is due to the second symmetric bending resonance. Both elastomers have a bulk modulus close to that of water.





VIEWGRAPH 3

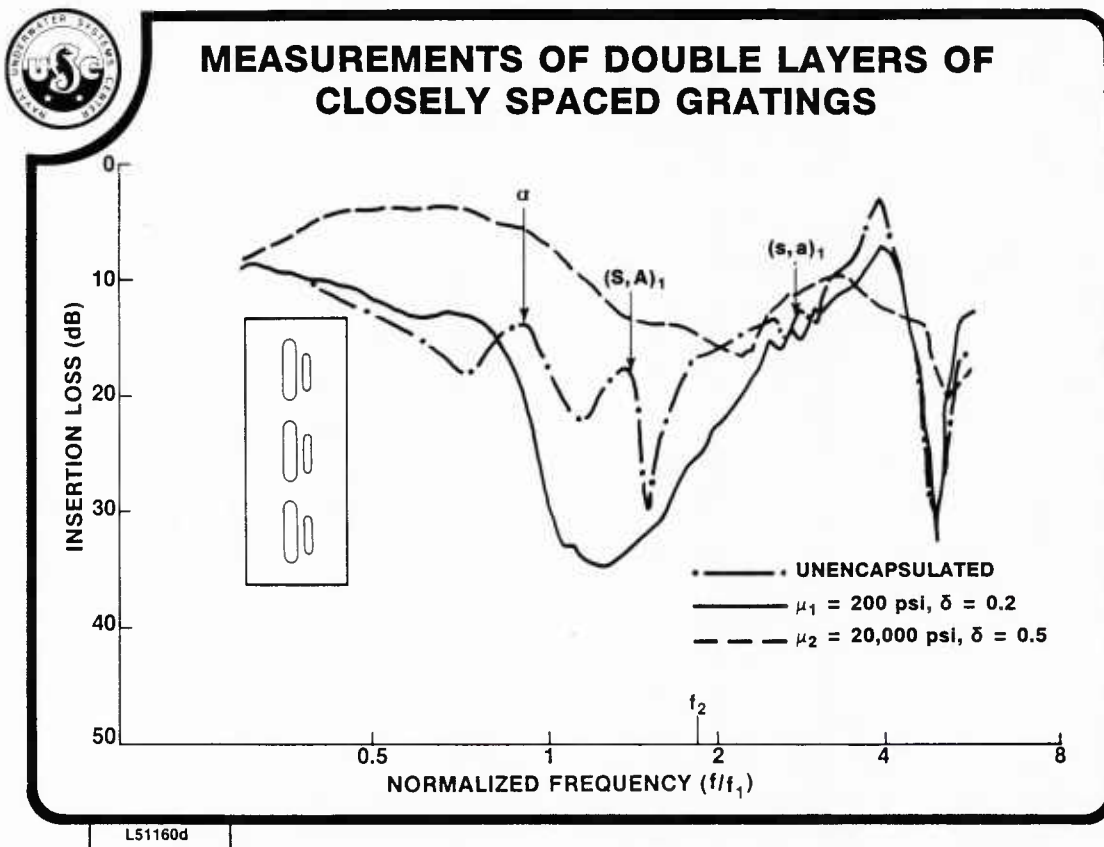
The performance of the smaller tube grating to be used in combination with the larger tube grating is presented. The fundamental compliant mode of the smaller tubes ( $f_2$ ) is equal to  $1.8f_1$ . Because mass loading is more significant for the wider spaced smaller tubes, the insertion loss maximum are lower in frequency than the in-air compliant resonance of the individual elements ( $f_2$ ). With wider spaced gratings, the bandwidth of insertion loss is narrower. The performance changes with encapsulation are similar to that for the larger tube grating.



VIEWGRAPH 4

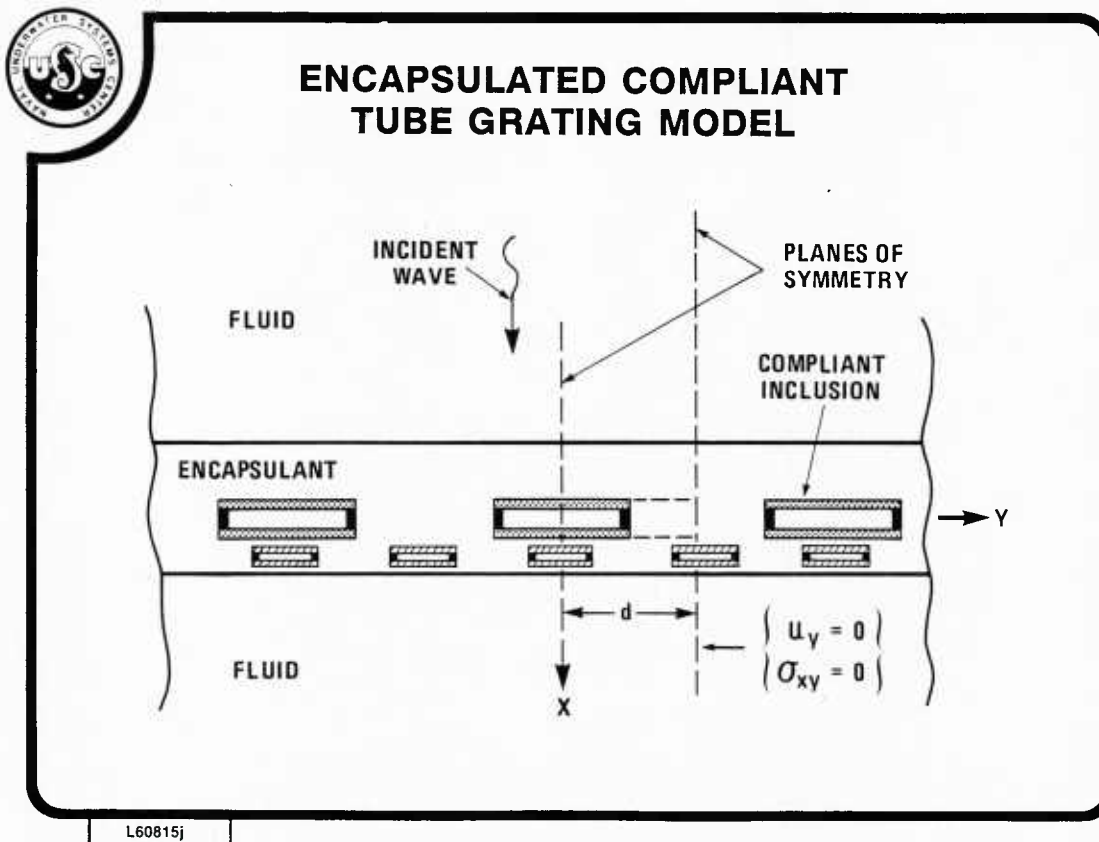
The two grating combination of the above single layers was measured for wide separation of  $\lambda_1/13$  where  $\lambda_1$  is the wavelength in water at the fundamental compliant structural mode of the larger tubes. The additional bandwidth obtained from the combination is significant. The transmission maximum at  $\alpha$  is due to a resonance of the compliance of the gratings with the inner layer mass. The low stiffness elastomer has a minimum effect on the performance with respect to the unencapsulated tubes, but the high stiffness encapsulant again shifts the maximum bandwidth of insertion loss to higher frequencies and degrades performance.





VIEWGRAPH 5

For the closely spaced gratings of separation  $\lambda_1/82$ , the fundamental insertion loss bandwidth is severely degraded. This decrease in the fundamental bandwidth is caused by the nearfield excitation of the second noncompliant bending mode  $(S, A)_1$  of the larger tubes and the enhanced motion of the radiating rigid body mode. Because the decrease in mass between the two gratings raises the resonance frequency of the first transmission resonance, increased insertion loss with respect to the widely spaced gratings is found at low frequencies. The low stiffness elastomer actually improves the performance bandwidth with respect to the gratings in fluid. Excitation of the antisymmetric mode of the smaller tubes is designated by  $(s, a)_1$ . The higher stiffness encapsulant again degrades performance.



VIEWGRAPH 6

A schematic representation of multiple compliant tube gratings embedded in a viscoelastic layer is shown for a normally incident plane wave. A two dimensional representation is used to describe the interaction. The portion of the incident wave which enters the layer undergoes multiple reflections at both the tube and elastic-fluid boundaries. Some of this energy is absorbed and some is transmitted through the layer. Because of bending and rigid body translational motion of the tubes, shear waves are generated even at normal incidence. With the symmetry in the grating arrangement, the solution reduces to satisfying the boundary conditions between the planes of symmetry. The boundary condition in the fluid at the symmetry planes is that the transverse velocity is zero. In the elastomeric material, the additional boundary condition is zero transverse shear at the symmetry planes.



## FIELD EQUATIONS

### INCIDENT AND REFLECTED PRESSURE WAVES

$$P = e^{ik_0 x} + \sum_{n=0}^{\infty} R_n e^{-ik_n x} \cos \alpha_n y$$

$$k_n^2 = k_0^2 - \alpha_n^2; \alpha_n = \frac{n\pi}{d}$$

### DISPLACEMENT POTENTIALS FOR DILATATIONAL & SHEAR WAVES

$$\phi_j = \sum_{m=0}^{\infty} \left\{ A_m^{(j)} e^{ik_{mp} x} + B_m^{(j)} e^{-ik_{mp} x} \right\} \cos \alpha_m (y - c_j)$$

$$A_j = \sum_{m=0}^{\infty} \left\{ C_m^{(j)} e^{ik_{ms} x} + D_m^{(j)} e^{-ik_{ms} x} \right\} \sin \alpha_m (y - c_j)$$

$$k_{mp}^2 = k_p^2 - \alpha_m^2; k_{ms}^2 = k_s^2 - \alpha_m^2; \alpha_m = \frac{m\pi}{d - c_j'}$$

$k_p \equiv$  complex dilatational wavenumber

$k_s \equiv$  complex shear wavenumber

### TRANSMITTED PRESSURE WAVES

$$P_T = \sum_{n=0}^{\infty} T_n e^{ik_n x} \cos \alpha_n y$$

L60815d

#### VIEWGRAPH 7

The total pressure in the fluid above the elastomer is the sum of the incident plane wave and an infinite series of reflected waves.  $R_n$  represents an unknown scattering coefficient. The wavenumber of the  $n$ th reflected wave, namely  $k_n$ , is real when  $k_0$ , the fluid wavenumber, is greater than the grating parameter  $\alpha_n$ . In this case, the reflected wave propagates away from the grating into the fluid. For  $k_0$  less than  $\alpha_n$ ,  $k_n$  is imaginary and an evanescent wave propagates nearly parallel to the grating and decays exponentially away from the grating. In the assumed linear viscoelastic layer, the scalar and vector displacement potentials for the dilatational and shear waves are given as infinite series of inhomogeneous waves traveling in both directions. The dilatational and shear wavenumbers  $k_p$  and  $k_s$  are assumed complex. The constants  $c_j$  and  $c_j'$  are determined

by the geometry.  $A_m$ ,  $B_m$ ,  $C_m$ , and  $D_m$  are scattering coefficients determined by the boundary conditions. In the viscoelastic interstice between tubes, the transverse velocity and transverse shear stress are assumed zero at the tube-elastomer abutment. Of particular interest in this presentation is the calculation of the transmitted pressure. For grating spacing less than a wavelength in the fluid, the transmitted pressure in the field is determined by  $T_0$  which is the scattering coefficient of the single transmitted propagating wave.



## CLAMPED END CONDITIONS

### SYMMETRIC

$(s,s)_0$

$(s,s)_1$

$$W_q(y) = 0, \quad \frac{dW_q(y)}{dy} = 0 \quad \text{for } y = d'_q \pm b_q$$

$$W_q(y) = \sum_{s=0}^{\infty} W_s [ \cos k_s (y - d'_q) + C_s \cosh k_s (y - d'_q) ]$$

$$k_s = \frac{(2s + \frac{3}{2})\pi}{2b_q}, \quad 2b_q = \text{LENGTH OF } q\text{th PLATE}$$

$$C_s = \frac{-\cos k_s b_q}{\cosh k_s b_q}$$

L51071b

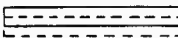
### VIEWGRAPH 8

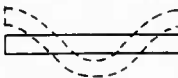
The plates are assumed to obey thin plate theory. The compliant symmetric modes of the compliant tube whose motion results in a net volume displacement are approximated by a sum of cosines and hyperbolic cosines. The designation  $(s,s)$  implies symmetric about the major and minor axes. Mode shaped  $(s,s)_0$  is the fundamental and  $(s,s)_1$  is the second symmetric bending mode.



## GUIDED END CONDITIONS

MINOR AXIS SYMMETRIC,  
MAJOR AXIS ASYMMETRIC

$(s, a)_0$  

$(s, a)_1$  

$$\frac{dW_q(y)}{dy} = 0, \quad \frac{d^3 W_q(y)}{dy^3} = 0 \quad \text{for } y = d'_q \pm b_q$$

$$W_q(y) = \sum_{s=0}^{\infty} W_s \cos k_s (y - d'_q)$$

$$k_s = \frac{s \pi}{b}$$

L51071d

### VIEWGRAPH 9

The modes that are symmetric about the minor axis but antisymmetric about the major axis  $(s, a)$  include the rigid body mode  $(s, a)_0$  and the "banana" shaped mode  $(s, a)_1$ . These modes are described mathematically with guided end conditions or zero slope and zero transverse shear at the ends. The  $(s, a)_1$  mode was shown in the experimental data to be excited by evanescent waves for closely packed gratings and it degrades insertion loss performance.





## **BOUNDARY CONDITIONS**

### **FLUID - ELASTOMER INTERFACES**

- (1) ZERO SHEAR STRESS**
- (2) NORMAL DISPLACEMENT CONTINUOUS**
- (3) NORMAL STRESS EQUAL NEGATIVE PRESSURE IN FLUID**

### **ELASTIC - ELASTIC REGION BOUNDRIES**

- (1) NORMAL AND TANGENTIAL DISPLACEMENTS CONTINUOUS**
- (2) NORMAL AND TANGENTIAL STRESSES CONTINUOUS**

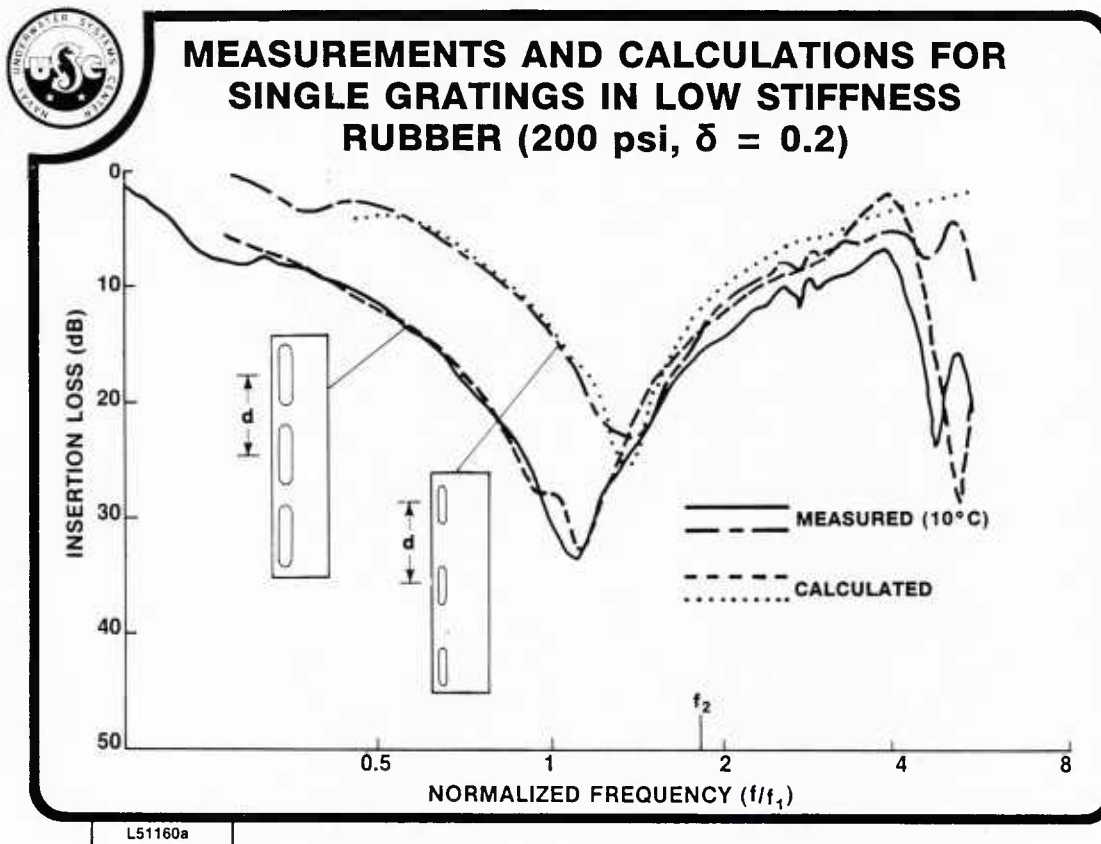
### **PLATE - ELASTOMER INTERFACE**

- (1) NORMAL AND TANGENTIAL DISPLACEMENTS CONTINUOUS**
- (2) THIN PLATE EQUATION**

L60815f

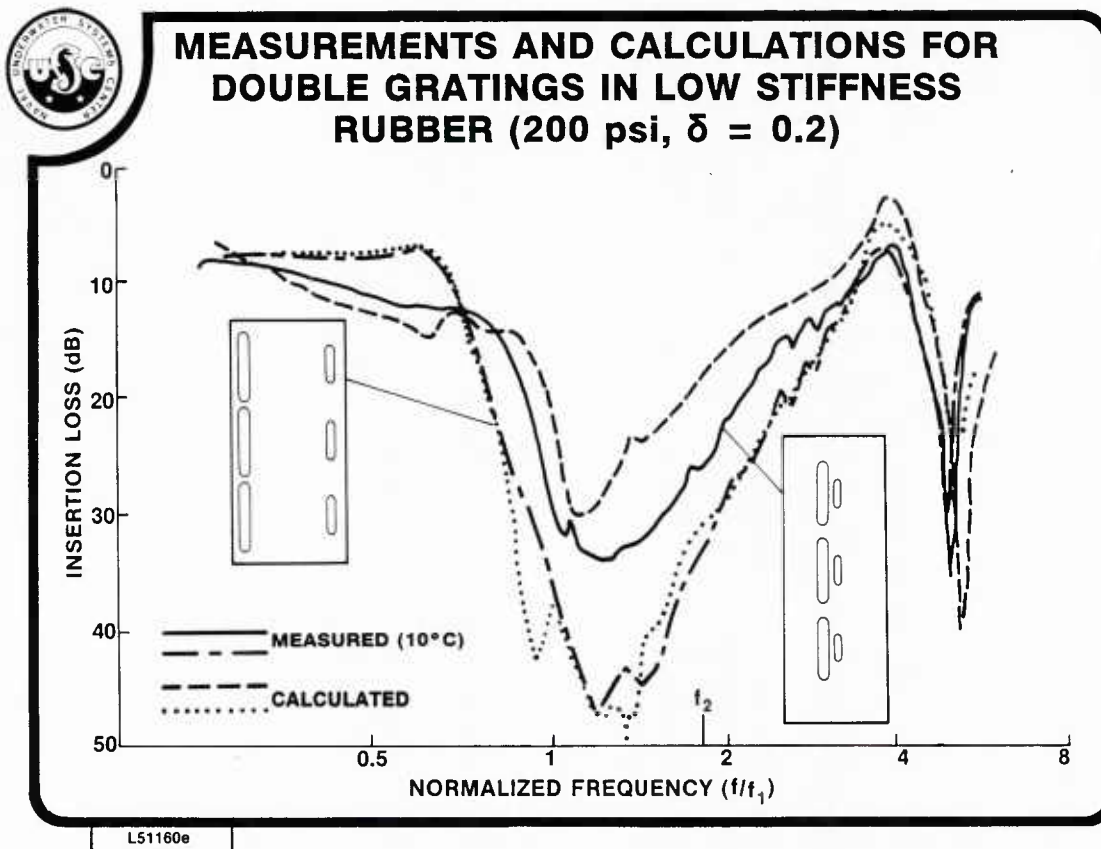
### **VIEWGRAPH 10**

The boundary conditions to be satisfied at the fluid-elastomer and elastic-elastic interfaces are those common for plane strain problems. The continuity of tangential displacement at the plate-elastomer boundary is derived by assuming inextensional motion of the plate. A system of linear equations is formed by matching the boundary conditions. Solutions of the simultaneous equations arising from truncation of the infinite sets are used to determine the scattering coefficients.



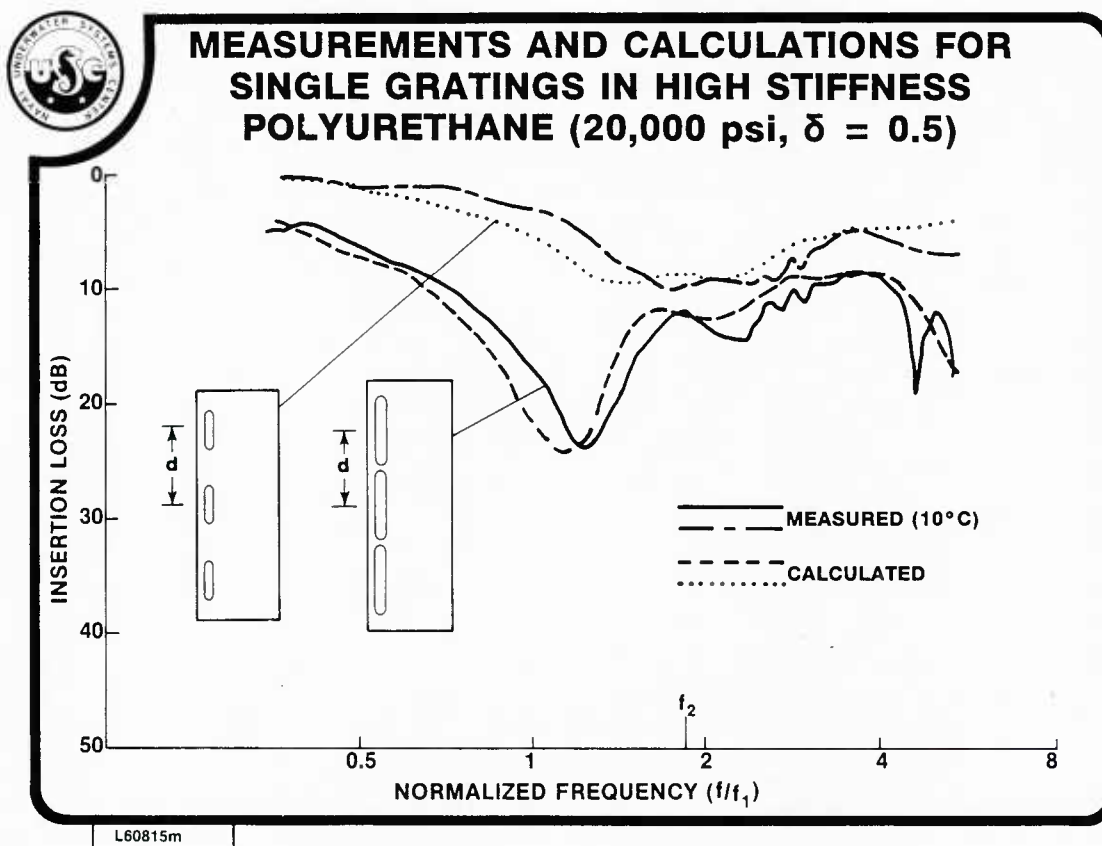
VIEWGRAPH 11

A comparison of measurements and calculations of insertion loss are shown for both the larger tubes in a dense packing and the smaller tubes in a sparse packing. Both gratings have a periodicity of  $d$ . The Young's moduli of the materials were measured with a Bruel and Kjaer apparatus where a strip is coated on a metal bar and the resonances of the uncoated and coated bar are compared to obtain the complex-valued material properties. No measurement was available for the bulk or dilatational modulus of the materials but in this frequency range, the calculations were not sensitive to say a 50% variation in the bulk modulus. A bulk modulus similar to water was assumed for these materials. As seen in the comparisons, for both cases excellent agreement is found for the single gratings.



VIEWGRAPH 12

With this comparison, the differences in insertion loss performance due to spacing between gratings is dramatically apparent. Again agreement between the predicted and measured insertion loss for both cases is good. The low frequency performance is better for the closely packed gratings because the transmission resonance seen at about  $0.7f_1$  for the widely spaced gratings shifts to about  $0.9f_1$ .

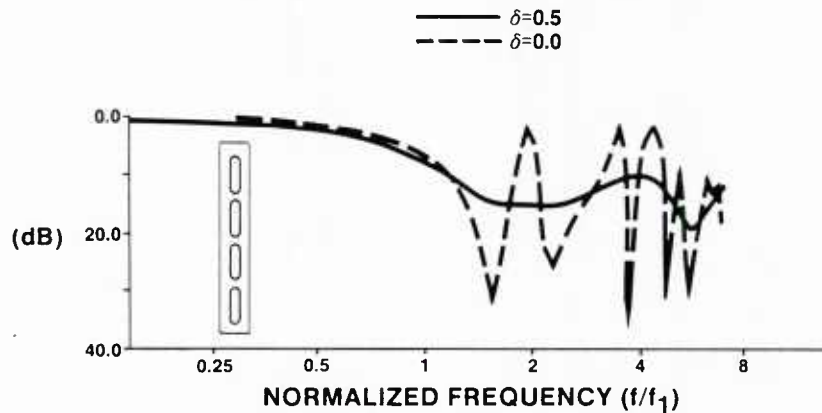


VIEWGRAPH 13

Although good agreement is seen between the experimental data and predictions, it was found that the calculations were sensitive to small variations of the thickness of the thin covering of the asymmetric layer configuration. With a very thin layer of the polyurethane on one side of the tubing, the additional stiffness effects can be mitigated. Neither configuration would perform satisfactorily as a decoupler but might be more appropriately used as an anechoic absorptive material.



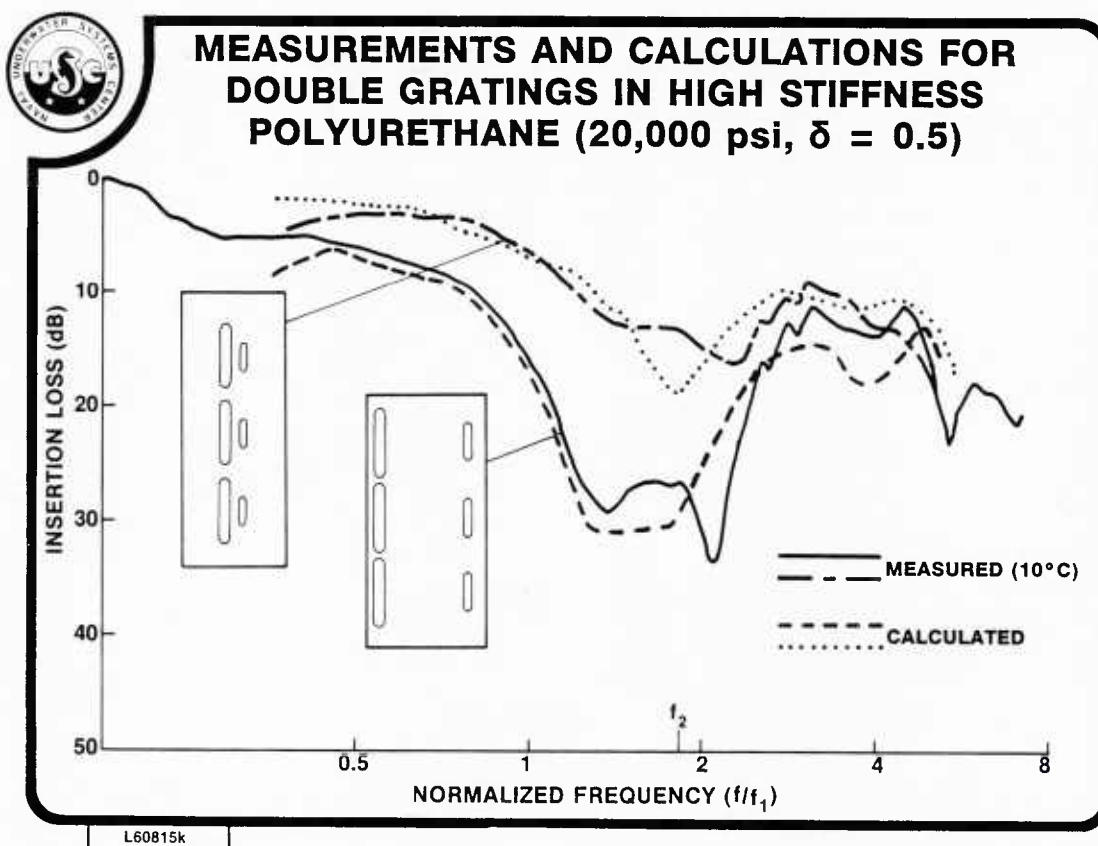
# **CALCULATIONS OF INSERTION LOSS FOR LOSS FACTOR VARIATIONS IN HIGH SHEAR MODULUS MATERIAL ( $\mu = 20,000$ psi)**



L60815a

VIEWGRAPH 14

The large oscillations in insertion loss in the undamped material are due to thickness resonances of the elastic layer from the shear waves generated by the motion of the tubes. The damping in the viscoelastic material converts these shear waves to heat and thus smooths the response of the insertion loss curves.



VIEWGRAPH 15

Differences between insertion loss performance between the closely packed and widely spaced gratings are more significant for the higher stiffened polyurethane encapsulant. The difference between calculations and experimental data for the higher stiffness material may be partially due to uncertainties in determination of the shear modulus. In the rubber-glass transition region of this polymer, small uncertainties in temperatures result in significant uncertainties in determination of the material properties. When these measurements were performed at the NUSC Dodge Pond facility, a temperature gradient was measured across the panel depth.



## CONCLUSIONS

Good agreement has been found between predictions of an analytical model and measurement of insertion loss from multiple gratings of compliant tubes in a viscoelastic layer immersed in water. For single gratings, low shear modulus materials were shown to have minimum effect with respect to in fluid measurements; however, high shear modulus polymers both raise the frequencies and decrease the quality factor of the array resonances. With increased stiffness of the encapsulant, more energy is transmitted through the layer. The loss factor of the material was shown to minimize the effects of layer thickness resonances. For multiple gratings in close proximity, the low stiffness encapsulant was shown to mitigate the near field excitations of the antisymmetric guided modes and thereby improve baffling performance.

# INITIAL DISTRIBUTION LIST

Addressee	No. of Copies
ONR (ONR-100, -410, -425AC)	3
NRL (L. Dragonette)	1
NRL, USRD (A. L. Van Buren, A. Rudgers)	1
NORDA (M. Werby)	1
NCSC (R. Hackman)	1
NAVSURFWPNCEN (Code U31, G. Gaunard, K. P. Scharnhorst, W. Madigosky)	3
DWTNSRDC BETH (Code 1902.5, J. Dlubac, W. Reader; 1965, M. Rurerman, F. Desiderati)	4
NAVPGSCOL	1
Center for Naval Analyses (Acquisition Unit)	1
BB&N, Inc. (J. Young)	1
Honeywell, Inc., Marine Systems Division, Seattle Washington (Murray Simon)	1
Cambridge Collaborative (James Moore)	1
DTIC	2

U227684